Electronic Supplementary Material (ESI) for Catalysis Science & Technology.
This journal is © The Royal Society of Chemistry 2018

Electronic Supplementary Information

How the distribution of reduced vanadium centers affects structure and stability of the MoVO$_x$ material

Wenqing Li,[a,§] Torstein Fjermestad,[a,§] Alexander Genest,[a] Notker Rösch*[,a,b]

Content

---

[a] Institute of High Performance Computing, Agency for Science, Technology and Research, 1 Fusionopolis Way, #16-6 Connexis, Singapore 138632
[b] Department Chemie and Catalysis Research Center, Technische Universität München, 85747 Garching, Germany, * E-mail: roesch@mytum.de

[§] W.-Q.L. and T.F. contributed equally to this work.

1 Computational details

To model the $MoVO_x$ material we applied electronic structure calculations at the density-functional theory (DFT) level to periodic models with a single layer per bulk unit cell. We used the unrestricted Kohn-sham approach, specifically the hybrid functional B3LYP[1] augmented by the D2 dispersion correction[2] as implemented in the code CRYSTAL14.[3] This hybrid exchange-correlation approach was chosen because it offers a notable reduction of the self-interaction error (SIE) compared to GGA functionals,[4] often selected for describing the electronic structure of solid materials. In consequence, valence *d* electrons are described as sufficiently localized at V centers, being most relevant in this work. Thus, this method offers an adequate description of the oxidation state and its changes in oxidation processes.[5] Previously, we showed for transition metal oxo complexes,[5] with a single metal center (V, Mo and Bi), that B3LYP reaction energies of oxidation processes agree well, within 21 kJ mol^{-1} on average, with the results of CCSD(T) calculations.

CRYSTAL14 employs Gaussian-type basis sets. We selected all-electron split-valence basis sets where feasible: 86-411d31G for V,[6] 8-411d1 for O,[7] and 5-11G* for H.[8] For Mo, we chose the valence basis set[9] 311(d31)G in combination with a Hay-Wadt small-core effective core potential for representing the core $1s^2 2s^2 2p^6 3s^2 3p^6 3d^{10}$.[10] The five threshold parameters ITOL1 to ITOL5 that control the accuracy of evaluating Coulomb and exchange integrals were set to 7, 7, 7, 9, and 30.[11] The SCF convergence threshold was set to 10^{-7} a.u. We optimized both the unit cell and the atomic positions within the unit cell, using the following thresholds: (*i*) atomic displacements – RMS value at most 1.2×10^{-3} a.u, largest value at most 1.8×10^{-3} a.u.; (*ii*) atomic displacement gradients – RMS value at most 3.0×10^{-4} a.u., largest value at most 4.5×10^{-3} a.u. Integrations over the Brillouin zone were carried out using a 1×1×4 k-point mesh.[12] A test calculation with the denser 2×2×4 k-grid for the most and the least stable configuration resulted in only marginal changes of at most 0.13 kJ mol^{-1}. The structures of the 14 configurations (representing the selected distributions of 6 reduced centers among the 10 V centers) were optimized without any symmetry restrictions.

The spin orientations of the unpaired electrons were all kept parallel, thus computing a ferromagnetic-type configuration. For structures **1** to **6**, belonging to the space groups Pba2 and P2, we also probed antiferromagnetic arrangements of configurations by reversing the spin orientation of three of the reducing electrons; see Table S1. The resulting reductions of the total energy were calculated at 3–8 kJ mol^{-1}. For the same structures **1** to **6**, we also checked the effect of antiferromagnetic-type coupling between adjacent layers by constructing two-layer bulk unit cells. In these calculations, we employed a 1×1×2 k-point mesh, to keep the density of k-points constant. These two-layer structures with antiferromagnetic coupling resulted in energy changes from -0.03 kJ mol^{-1} (**1**) to 0.32 kJ mol^{-1} (**4**) per unit cell We deemed these energy variations due to “spin flipping” to be insignificant compared to the energy variations due to different distributions of the reducing electrons. Therefore, we considered only ferromagnetic configurations in this work.

For structures **1** and **2**, we estimated the interaction energy between the layers of the material. To this end, we carried out single-point calculations on one-layer “slab” models which had been constructed from the optimized bulk models by adding 500 Å of “vacuum” in *c* direction. Then the interaction energy may be estimated at $E_{\text{int}} = (E_{\text{slab}} – E_{\text{bulk}}) / 2$ where E_{slab} is the energy of the slab model at the bulk geometry and E_{bulk} is the energy of the bulk structure. The factor ½ accounts for the fact that two surfaces are created upon constructing the slab. The resulting interaction energies were 1396 kJ mol^{-1} (**1**) and 1462 kJ mol^{-1} (**2**). Thus, the interaction energy per oxo group is ~35 kJ mol^{-1} where the dispersion correction contributes about half of this value.

The optimized lattice constants, Table S1, agree well with experimental results.[13] The maximum deviation, 1.8 %, between theoretical and experimental values occurs for the lattice constant *c*.

To obtain the projected density of states (pDOS), we employed a refined mesh of 2×2×8 k-points for the integrations over the Brillouin zone. For calculating the DOS, the energy spacing $\Delta\varepsilon \approx 1$ kJ mol^{-1} was used, invoking Legendre polynomials to represent the DOS.[14] To facilitate the analysis of pDOS peak energy values, we calculated for each gap state the energy ε as the density-weighted average position over the corresponding peak:

$$\varepsilon = \frac{1}{N_T} \sum_i w_i \varepsilon_i \quad \text{where} \quad N_T = \sum_i w_i \quad \text{and} \quad w_i = D(\varepsilon_i) \Delta\varepsilon$$

$D(\varepsilon_i)$ is the density of states at energy ε_i, and N_T is the DOS summed for that gap state.

Reference structure 15. For discussing polaron-induced lattice distortions, we optimized the structure of the material $Mo_{30}V_{10}O_{112}$ with all metal centers fully oxidized. This choice implies a charged model, +6 *e* per unit cell. To neutralize the system, a uniform background charge of opposite sign was introduced.[15] The optimization was started from the optimized structure of **1**, S1abS3abcd, relaxing only the atomic positions in the unit cell, but keeping the lattice parameters fixed. We refer to this configuration as structure **15**.

2 Splitting of gap states

In the band gap, the energies of occupied *d* states of reduced V centers vary, depending on the environment of the center, Figure S5. If the reduced V centers are giving rise to a polaron-polaron interaction (pol-pol, see main text), then the gap states from reduced V centers split and broaden, Figure S5 and Table S2. For example, the pDOS features of reduced V centers at sites S1a and S1b in configuration **2**, S1abS7abcd, are narrower than those due to the states of V at sites S7abcd. The two V centers of the pentameric unit are undergoing a pol-pol interaction mediated via site S2. In contrast, no such pol-pol interaction is found for the reduced V centers at sites S1a and S1b. Further examples of this type of pDOS peak splitting are the gap states of reduced V centers at sites S1b in configuration **3**, S1abS3abS7cd, and S1a in configuration **4**, S1abS3cdS7cd.

References

1. A. D. Becke, *J. Chem. Phys.*, 1993, **98**, 5648.
2. S. Grimme, *J. Comput. Chem.* , 2006, **27** 1787.
3. R. Dovesi, R. Orlando, A. Erba, C. M. Zicovich-Wilson, B. Civalleri, S. Casassa, L. Maschio, M. Ferrabone, M. De La Pierre and P. D'Arco, *Int. J. Quantum Chem.*, 2014, **114**, 1287.
4. M. Lundberg and P. E. M. Siegbahn, *J. Chem. Phys.*, 2005, **122**.
5. S. Dinda, C.-c. Chiu, A. Genest and N. Rösch, *Comput. Theor. Chem.*, 2016, **1101**, 36.
6. E. Ruiz, M. Llunell and P. Alemany, *J. Solid State Chem.*, 2003, **176**, 400.
7. T. Bredow, K. Jug and R. A. Evarestov, *Phys. Status Solidi B*, 2006, **243**.
8. R. Dovesi, C. Ermondi, E. Ferrero, C. Pisani and C. Roetti, *Phys. Rev. B*, 1984, **29**.
9. F. Cora, A. Patel, N. M. Harrison, C. Roetti and C. Richard A. Catlow, *J. Mater. Chem.*, 1997, **7**.
10. P. J. Hay and W. R. Wadt, *J. Chem. Phys.*, 1985, **82**, 299.
11. R. Dovesi, V. R. Saunders, C. Roetti, R. Orlando, C. M. Zicovich-Wilson, F. Pascale, B. Civalleri, K. Doll, N. M. Harrison, I. J. Bush, P. D’Arco, M. Llunell, M. Causà and Y. Noël, *CRYSTAL14 User's Manual*, University of Torino, Torino, 2014, pp. 277-278.
12. H. J. Monkhorst and J. D. Pack, *Phys. Rev. B*, 1976, **13**.
13. S. Ishikawa, D. Kobayashi, T. Konya, S. Ohmura, T. Murayama, N. Yasuda, M. Sadakane and W. Ueda, *J. Phys. Chem. C*, 2015, **119**, 7195.
14. R. Dovesi, V. R. Saunders, C. Roetti, R. Orlando, C. M. Zicovich-Wilson, F. Pascale, B. Civalleri, K. Doll, N. M. Harrison, I. J. Bush, P. D’Arco, M. Llunell, M. Causà and Y. Noël, *CRYSTAL14 User's Manual*, University of Torino, Torino, 2014, p. 207.
15. R. Dovesi, V. R. Saunders, C. Roetti, R. Orlando, C. M. Zicovich-Wilson, F. Pascale, B. Civalleri, K. Doll, N. M. Harrison, I. J. Bush, P. D’Arco, M. Llunell, M. Causà and Y. Noël, *CRYSTAL14 User's Manual*, University of Torino, Torino, 2014, p. 69.

3 Tables

Table S1. Lattice parameters calculated for 14 distributions (configurations) of reduced V centers. Conf. designates the label of the structure. Cell vectors *a*, *b*, *c* in Å, angles α, β, γ in degree.

Space group	Conf.	Reduced centers[a,b]			Cell vector			Cell angle		
		S1	S3	S7	*a*	*b*	*c*	α	β	γ
	Exp.[c]				20.99	26.40	3.99	90.0	90.0	90.0
Pba2	**1**	***a***b	ab***cd***		21.04	26.45	4.06	90.0	90.0	90.0
	2	a***b***		a***b***c***d***	21.01	26.68	4.04	90.0	90.0	90.0
P2	**3**	a***b***	***ab***	cd	21.06	26.56	4.05	90.0	90.0	90.1
	4	***a***b	***cd***	cd	21.03	26.59	4.05	90.0	90.0	90.3
	5		a***b***c***d***	***c***d	21.18	26.46	4.04	90.0	90.0	90.1
	6		a***b***	***a***b***c***d	21.10	26.60	4.04	90.0	90.0	90.0
Pc	**7**	ab	ad	ad	21.05	26.61	4.04	90.1	90.0	90.0
	8	ab	ac	bd	21.07	26.58	4.04	90.0	90.0	90.0
	9	ab	ad	bc	21.03	26.59	4.05	89.9	90.0	90.0
	10	ab	ac	ac	21.07	26.63	4.03	90.0	89.9	90.0
	11		abcd	bc	21.19	26.47	4.04	89.9	90.0	90.0
	12		abcd	ac	21.19	26.48	4.04	90.0	90.0	90.0
	13		ad	abcd	21.11	26.60	4.04	90.0	90.0	90.0
	14		ac	abcd	21.10	26.62	4.04	90.0	90.0	90.0

[a] For each configuration, type and location of reduced V centers; see Figure 1. [b] Labels of centers rendered in italics+bold indicate V centers where the spin orientation was reversed when testing energy changes due to antiferromagnetic coupling. [c] Ref. 13.

Table S2. Density-of-state weighted average energy positions ε, kJ mol^{-1}, of gap states due to reduced V centers in the selected 14 configurations,[a] relative to the bottom of the conduction band.

Space group	Conf.	Reduced centers[b]			*E*									
		S1	S3	S7	S1a	S1b	S3a	S3b	S3c	S3d	S7a	S7b	S7c	S7d
Pba2	**1**	ab	abcd		-189	-188	-170	-170	-170	-170				
	2	ab		abcd	-211	-211					-159	-159	-159	-159
P2	**3**	ab	ab	cd	-176	-191	-149	-149					-123	-123
	4	ab	cd	cd	-199	-162			-147	-147			-121	-121
	5		abcd	cd			-165	-158	-162	-159			-121	-117
	6		ab	abcd			-134	-134			-113	-113	-118	-118
Pc	**7**	ab	ad	ad	-200	-200	-167			-167	-185			-186
	8	ab	ac	bd	-191	-191	-148		-148			-186	-186	
	9	ab	ad	bc	-198	-198	-161			-160		-186	-187	
	10	ab	ac	ac	-177	-177	-121		-121		-140		-141	
	11		abcd	bc			-166	-167	-167	-167		-167	-167	
	12		abcd	ac			-160	-173	-159	-173	-167		-166	
	13		ad	abcd			-147			-148	-126	-128	-128	-127
	14		ac	abcd			-125		-125		-114	-126	-113	-126

[a] For a detailed illustration of the distributions of reduced V centers, see Figures S2 to S4. [b] See Table 1 of the main text.

Table S3. Fitted parameters (kJ mol^{-1}) of models A, A', B, and C,[a] resulting standard error σ (kJ mol^{-1}), and coefficient of determination R^2.

Model	A	A'	B	C
C	6.64	1.56	-40.44	-33.11
$\varepsilon_{\text{S1-S3}}$	23.68	–	–	–
$\varepsilon_{\text{S3-S7}}$	11.70	–	–	–
ε_{sh}	–	16.06	14.66	15.76
ε_{pp}	–	–	10.27	8.15
ε_{aS2}	–	–	–	-20.08
σ	14.44	15.60	2.23	6.34
R^2	0.906	0.854	0.998	0.986

[a] Models A, A, and B fitted to the DFT energies of configurations **1** to **6**, model C fitted to the DFT energies of configurations **1** to **14**.

4 Figures

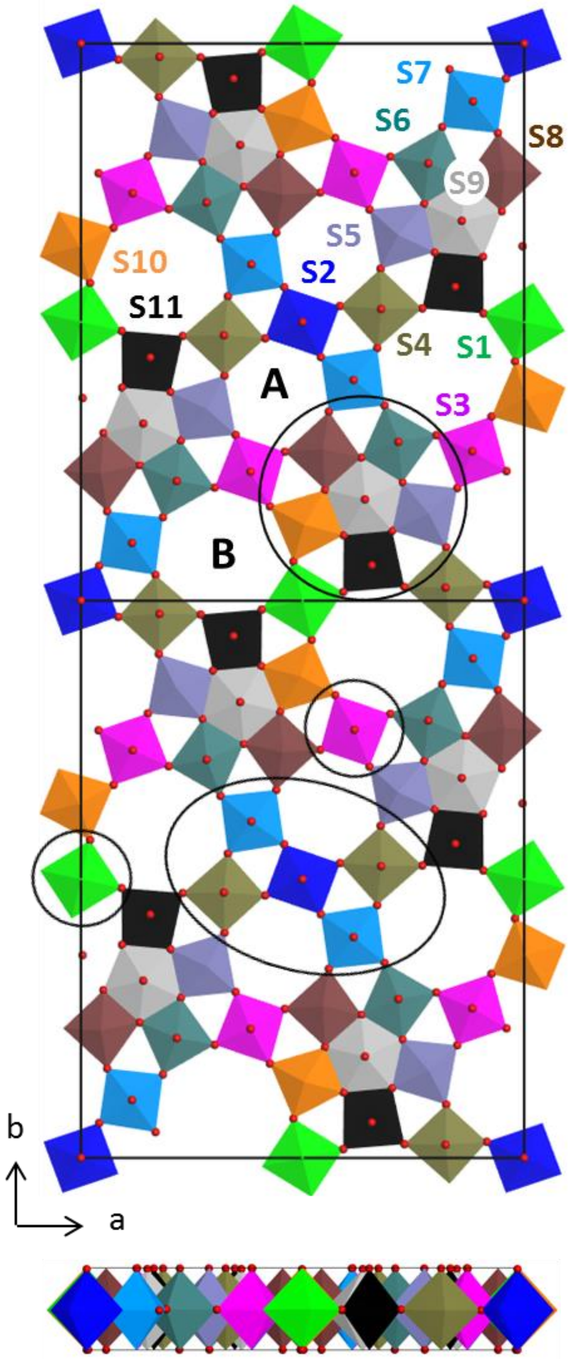

Figure S1. Polyhedral representation of the $Mo_{30}V_{10}O_{112}$ unit cell. Upper panel - Top view. Lower panel - side view. Labels S1, S3, S7 – vanadium moieties, S2, S4, S5, S6, S8, S9, S10, S11 – molybdenum moieties. Large circle – pentagonal unit, ellipse – pentameric unit, small circle – octahedral linker. Bold letters indicate hexagonal (A) and heptagonal (B) channels. Small red spheres (dots) – oxygen. S1 – green , S2 – blue, S3 – magenta, S4 – yellow green, S5 – light slate blue, S6 – light sea green, S7 – light blue, S8 – brown, S9 – light grey, S10 – dark orange, S11 – black.

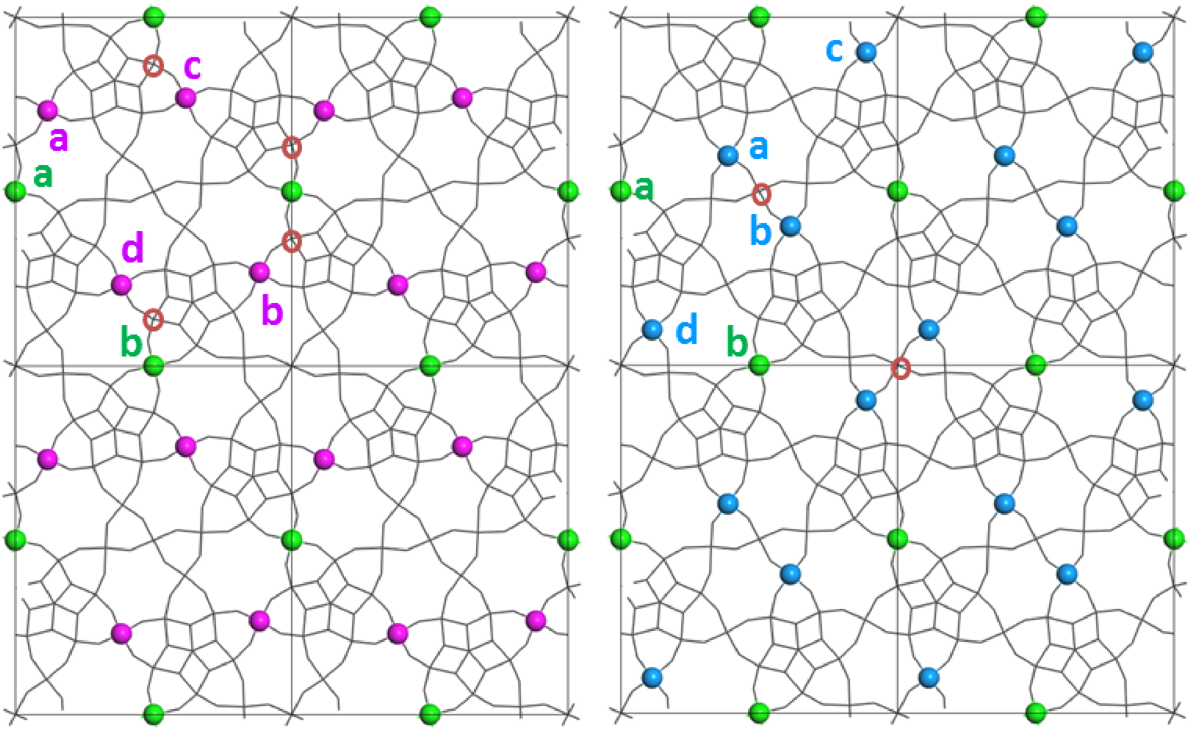

1 S1abS3abcd

2 S1abS7abcd

Figure S2. Configurations of six reduced V^{4+} centers in the unit cell $Mo_{30}V_{10}O_{112}$. Sketch of the *ab* plane for the two V^{4+} distributions of space group Pba2. Red circles – "squeezed Mo" center due to pol-pol interaction. S1 – green, S3 – magenta, S7 – light blue.

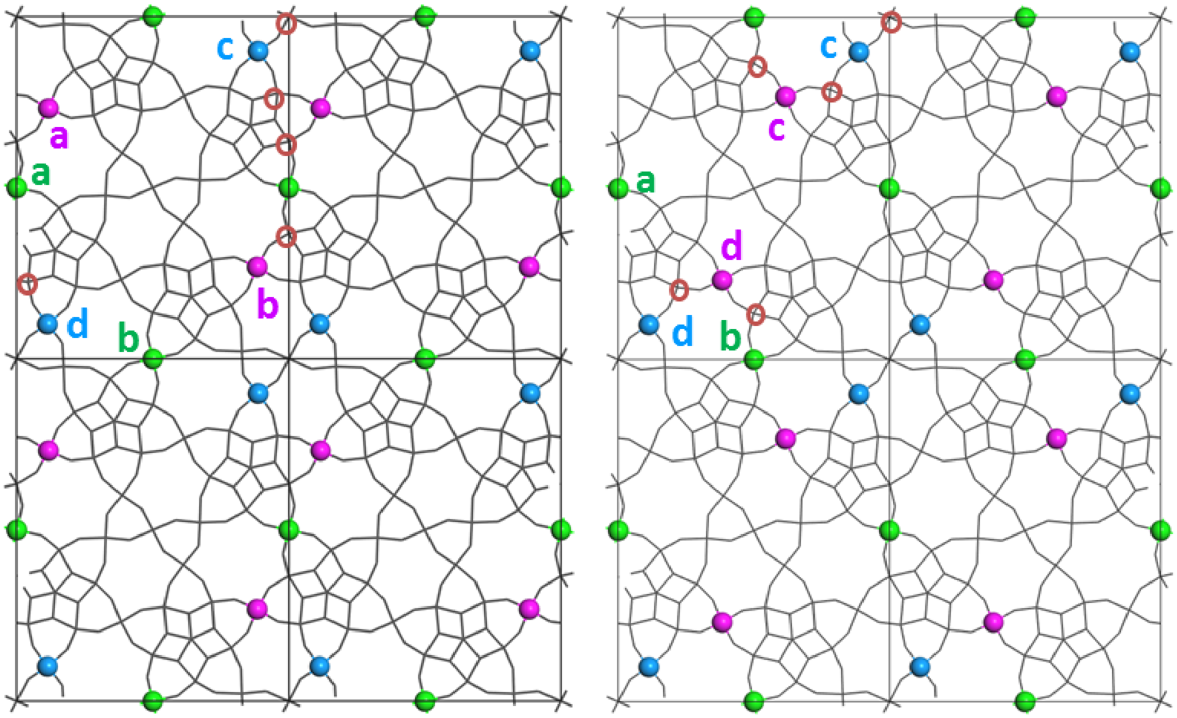

3 S1abS3abS7cd

4 S1abS3cdS7cd

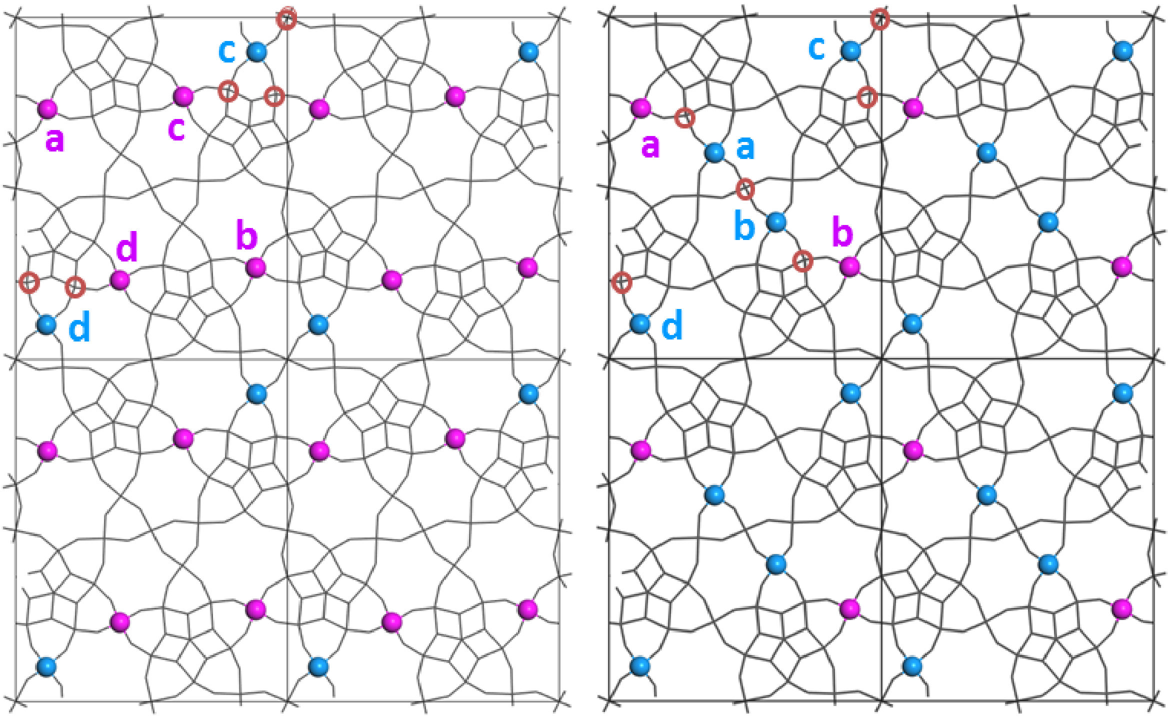

5 S3abcdS7cd

6 S3abS7abcd

Figure S3. Configurations of six reduced V^{4+} centers in the unit cell $Mo_{30}V_{10}O_{112}$. Sketch of the *ab* plane for the four V^{4+} distributions of space group P2. Lay-out as in Figure S2.

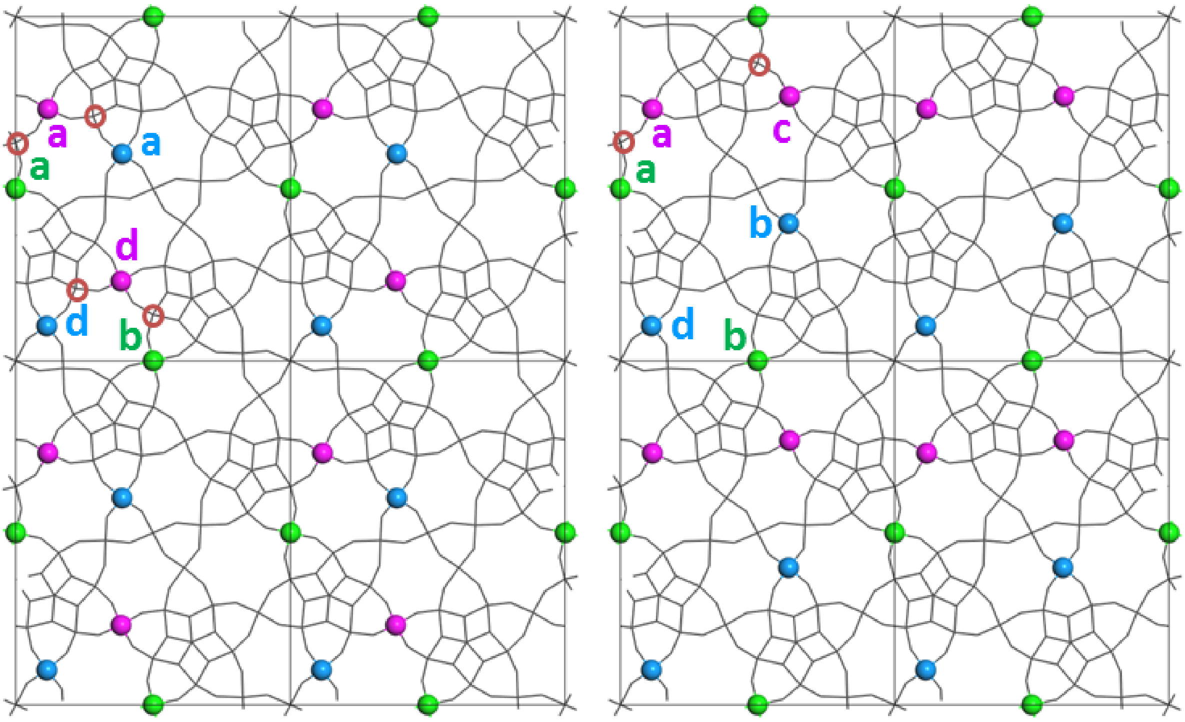

7 S1abS3adS7ad

8 S1abS3acS7bd

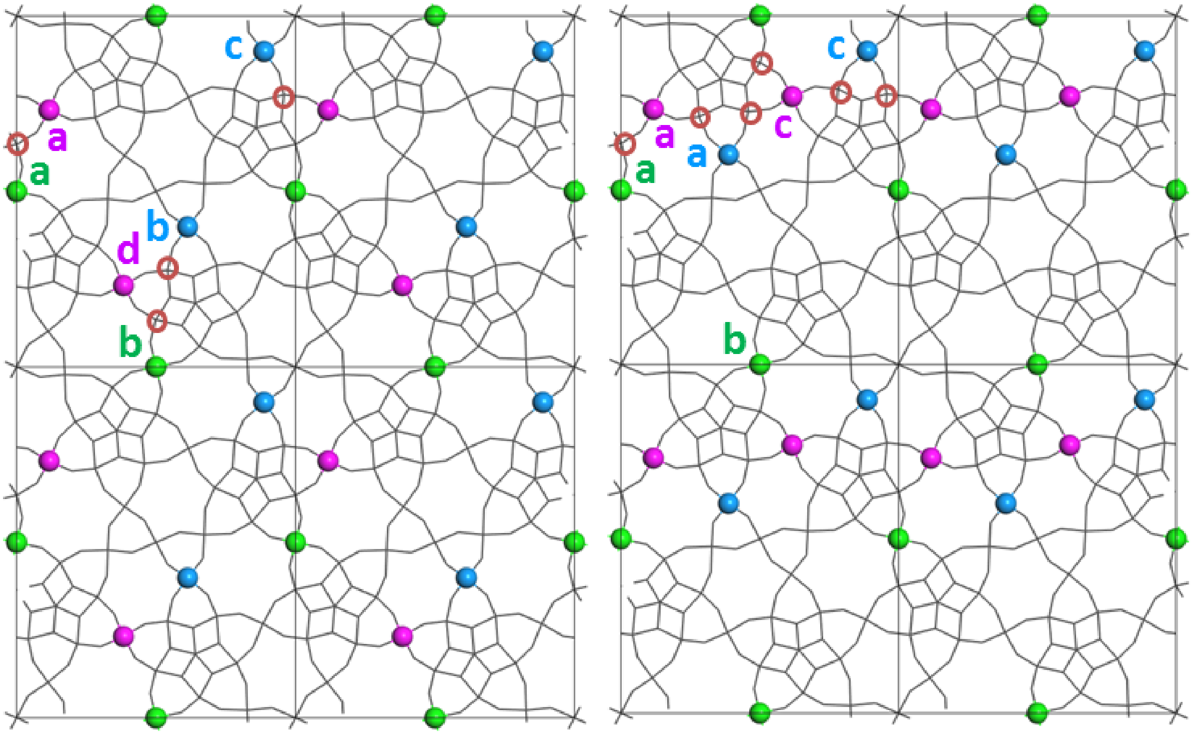

9 S1abS3adS7bc

10 S1abS3acS7ac

Figure S4. Configurations of six reduced V^{4+} centers in the unit cell $Mo_{30}V_{10}O_{112}$. Sketch of the *ab* plane for the eight V^{4+} distributions of space group Pc. Lay-out as in Figure S2.

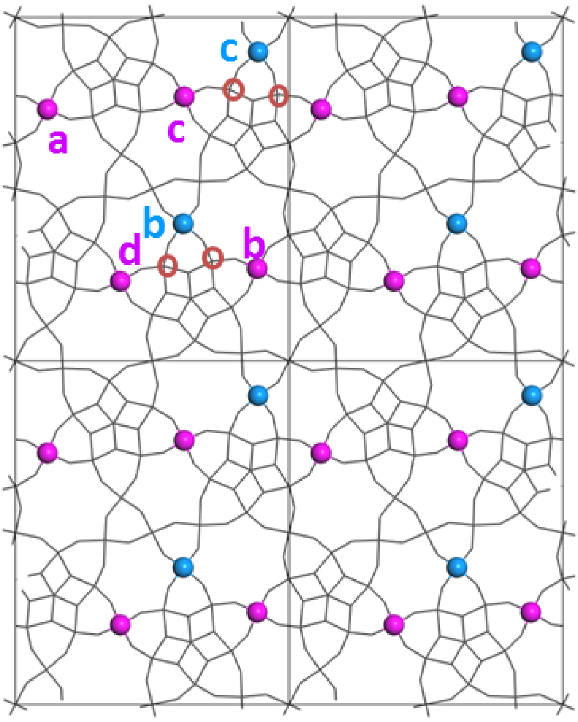

11 S3abcdS7cd

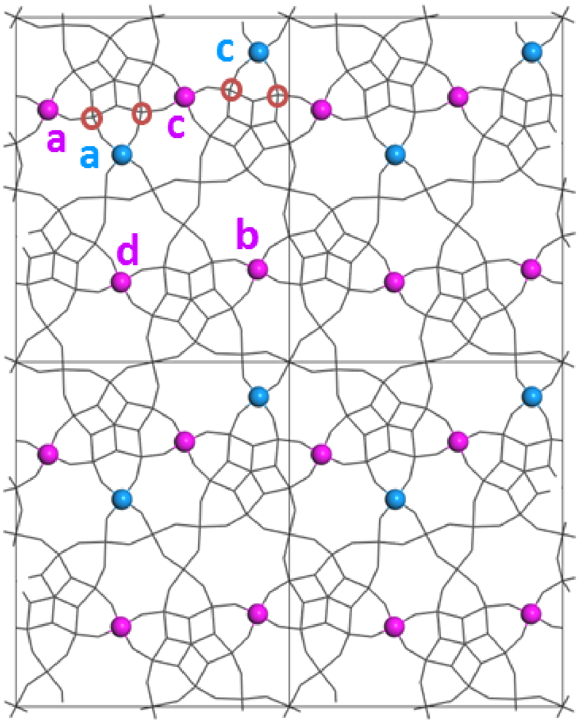

12 S3abcdS7ac

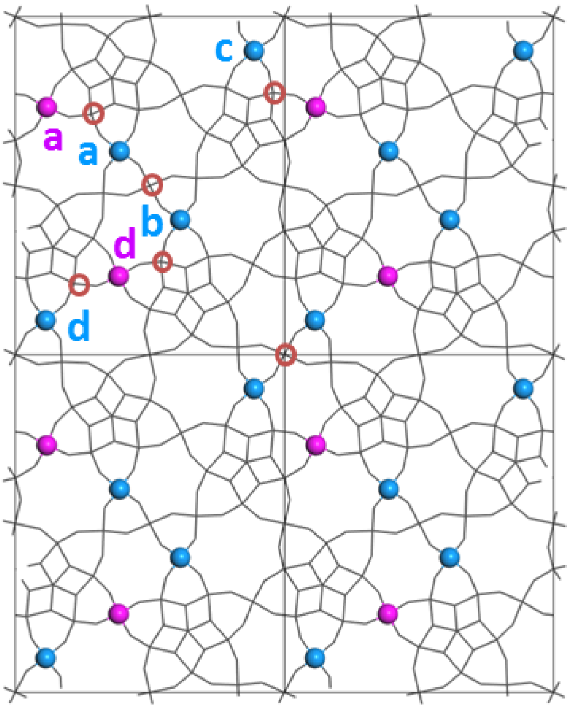

13 S3adS7abcd

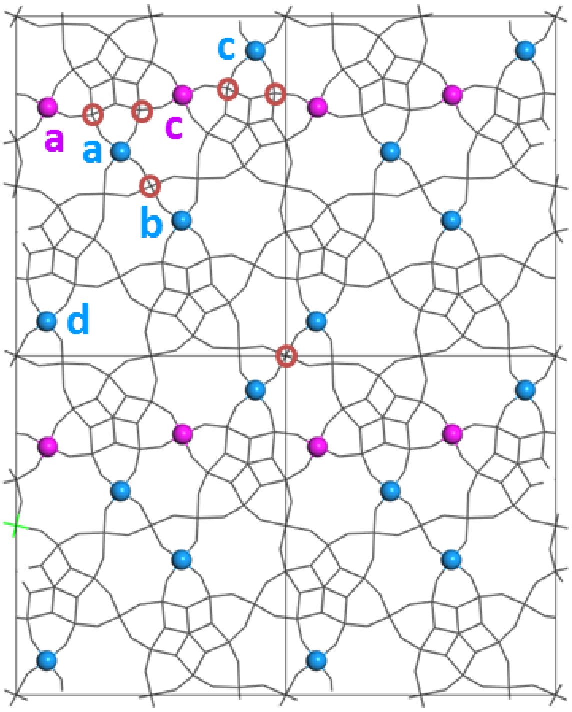

14 S3acS7abcd

Figure S4 (continued).

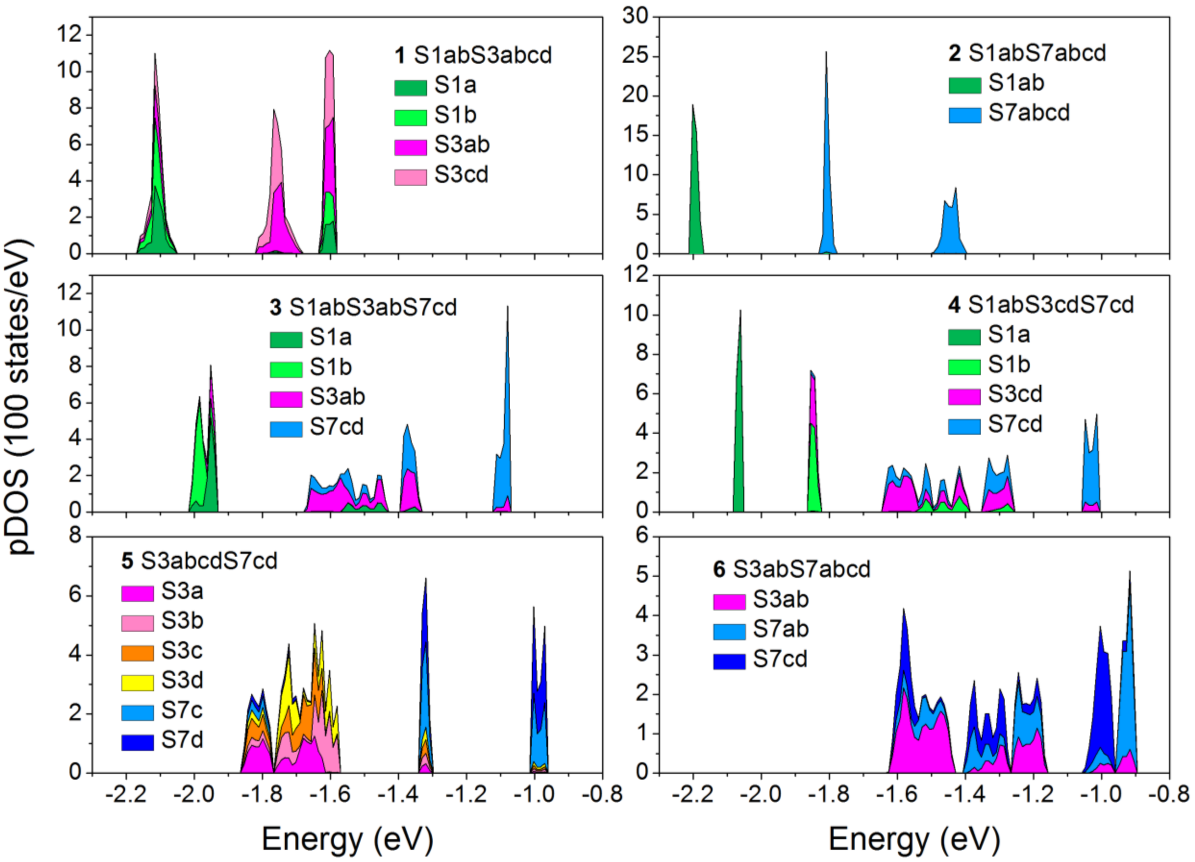

Figure S5. Projected density of states (pDOS) of reduced V centers for the six structures of the space groups Pba2 and P2. As energy reference, the bottom of the conduction band is set to zero. Color coding: S1 – green, S3 – magenta, S7 – blue. Non-equivalent centers at sites of the same type are colored in different shades of the base color, see legend. For the configuration labels "**1** S1abS3abcd" etc., see Table S2 and Table 1 of the main text.

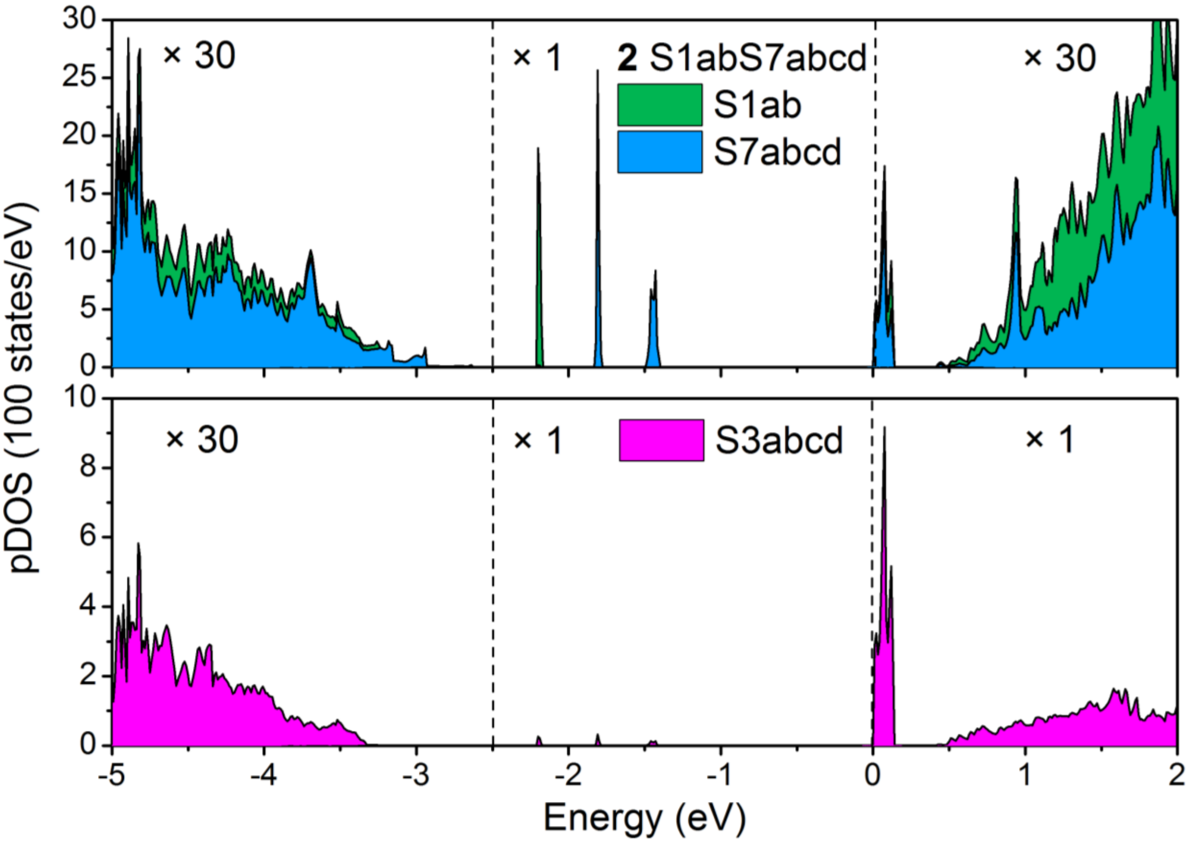

Figure S6. Projected density of states (pDOS) of reduced (top) and oxidized (bottom) V centers of configuration **2**. For clarity, the height of the original DOS (×1) is enlarged by a factor of 30 in the left- and right-most sections as indicated. Lay-out as in Figure S5.